Retinoschisin is linked to retinal Na/K-ATPase signaling and localization

Karolina Plössl[a], Melanie Royer[a], Sarah Bernklau[a], Neslihan N. Tavraz[b], Thomas Friedrich[b], Jens Wild[c], Bernhard H. F. Weber[a], and Ulrike Friedrich[a,*]

[a]Institute of Human Genetics and [c]Institute of Clinical Microbiology and Hygiene, University Hospital of Regensburg, University of Regensburg, 93053 Regensburg, Germany; [b]Institute of Chemistry, Technical University of Berlin, 10623 Berlin, Germany

ABSTRACT **Mutations in the *RS1* gene cause X-linked juvenile retinoschisis (XLRS), a hereditary retinal dystrophy. We recently showed that retinoschisin, the protein encoded by *RS1*, regulates ERK signaling and apoptosis in retinal cells. In this study, we explored an influence of retinoschisin on the functionality of the Na/K-ATPase, its interaction partner at retinal plasma membranes. We show that retinoschisin binding requires the β2-subunit of the Na/K-ATPase, whereas the α-subunit is exchangeable. Our investigations revealed no effect of retinoschisin on Na/K-ATPase–mediated ATP hydrolysis and ion transport. However, we identified an influence of retinoschisin on Na/K-ATPase–regulated signaling cascades and Na/K-ATPase localization. In addition to the known ERK deactivation, retinoschisin treatment of retinoschisin-deficient (*Rs1h*$^{-/Y}$) murine retinal explants decreased activation of Src, an initial transmitter in Na/K-ATPase signal transduction, and of Ca^{2+} signaling marker Camk2. Immunohistochemistry on murine retinae revealed an overlap of the retinoschisin–Na/K-ATPase complex with proteins involved in Na/K-ATPase signaling, such as caveolin, phospholipase C, Src, and the IP3 receptor. Finally, retinoschisin treatment altered Na/K-ATPase localization in photoreceptors of *Rs1h*$^{-/Y}$ retinae. Taken together, our results suggest a regulatory effect of retinoschisin on Na/K-ATPase signaling and localization, whereas Na/K-ATPase-dysregulation caused by retinoschisin deficiency could represent an initial step in XLRS pathogenesis.**

Monitoring Editor
Carl-Henrik Heldin
Ludwig Institute for Cancer Research

Received: Jan 30, 2017
Revised: Jun 2, 2017
Accepted: Jun 6, 2017

INTRODUCTION

X-linked juvenile retinoschisis (XLRS; Online Mendelian Inheritance in Man #312700) is a hereditary degenerative disease of the macula (Pagenstecher, 1913). The disease is characterized by a bilateral splitting of central retinal layers (foveal schisis), which leads to cystic degeneration of the retina. In addition, serious defects in visual signal transmission from photoreceptor to bipolar cells are evident (Khan *et al.*, 2001). Due to the X-chromosomal recessive mode of inheritance, XLRS predominantly affects young males, with prevalence estimates between 1:5000 and 1:20,000 (George *et al.*, 1995; Sauer *et al.*, 1997; Sikkink *et al.*, 2007).

XLRS is caused by mutations in the *RS1* gene on chromosome Xp22.1 (Sauer *et al.*, 1997). XLRS mouse models, generated via targeted disruption of the murine orthologue of *RS1*, the *Rs1h* gene, exhibit structural and functional changes that closely resemble the clinical features of XLRS patients (reviewed by Sikkink *et al.*, 2007; Molday *et al.*, 2012). This renders these mouse lines excellent disease models to study functional aspects of retinoschisin or explore novel therapeutic approaches (Sikkink *et al.*, 2007; Molday *et al.*, 2012).

The *RS1* gene is specifically expressed in photoreceptors and bipolar cells of the retina, as well as in pinealocytes of the pineal gland (Sauer *et al.*, 1997; Molday *et al.*, 2001; Takada *et al.*, 2006). It encodes a protein of 224 amino acids (aa) termed retinoschisin, which is exported as oligomers (Wu *et al.*, 2005; Tolun *et al.*, 2016). In the retina, it binds to plasma membranes of inner segments and plexiform layers (Molday *et al.*, 2007).

This article was published online ahead of print in MBoC in Press (http://www.molbiolcell.org/cgi/doi/10.1091/mbc.E17-01-0064) on June 14, 2017.

*Address correspondence to: Ulrike Friedrich (Ulrike.Friedrich@klinik.uni-regensburg.de)

The authors declare no conflicts of interest.

Abbreviations used: ATP, adenosine triphosphate; ERK, extracellular signal-regulated kinases; Erk1/2, Erk1 and Erk2; FACS, fluorescence-activated cell sorting; IP3, inositol trisphosphate; MAP, mitogen-activated protein; PP2, 4-amino-5-(4-chlorophenyl)-7-(dimethylethyl)pyrazolo[3,4-d]pyrimidine, a Src inhibitor; XLRS, X-linked juvenile retinoschisis.

The retinal Na/K-ATPase consisting of the two subunit isoforms ATP1A3 (α3) and ATP1B2 (β2) was identified as a direct interaction partner of retinoschisin (Molday *et al.*, 2007), anchoring retinoschisin to retinal plasma membranes (Friedrich *et al.*, 2011). Na/K-ATPases are integral membrane proteins found on the plasma membrane of essentially all eukaryotic cells (Geering, 2008). Their minimal functional unit is composed of two subunits (α and β), organized as a heterodimer (Geering, 2008). Na/K-ATPases primarily act as active ion pumps, transporting Na^+ and K^+ ions across the plasma membrane. Their function is indispensable for cellular homeostasis, as it maintains the cellular membrane potential, enables secondary active transport, regulates cell volume and osmolarity, and allows excitability of neuronal cells (for reviews, see Therien and Blostein, 2000; Geering, 2008; Friedrich *et al.*, 2016). Furthermore, Na/K-ATPases are important regulators of intracellular signaling cascades. On binding of cardiac glycosides such as ouabain, Na/K-ATPases induce mitogen-activated protein (MAP) kinase signaling, phosphatidylinositol 3-kinase (PI3K)/Akt signaling, and Ca^{2+} signaling (reviewed by Aperia *et al.*, 2016). Finally, Na/K-ATPases are implicated in intercellular adhesion (Krupinski and Beitel, 2009). In many tissues, Na/K-ATPases are associated with a specific class of transmembrane proteins—members of the FXYD family. These FXYD proteins modulate the Na/K-ATPase–mediated ion transport and intercellular adhesion (Geering, 2006; Tokhtaeva *et al.*, 2016).

Recently we showed that retinoschisin is a novel antiapoptotic regulator of MAP kinase signaling in the retina (Plössl *et al.*, 2017). However, the mechanism of signal transduction from externally bound retinoschisin to the MAP kinase cascade remained unresolved, although it might be reasonable to speculate that retinoschisin affects MAP kinase signaling via its effect on Na/K-ATPase–mediated signaling.

In this study, we show that retinoschisin specifically interacts with the β2-subunit of the retinal Na/K-ATPase. Retinoschisin binding showed no influence on active ion transport and substrate affinity of the retinal Na/K-ATPase but modulated Na/K-ATPase–regulated intracellular signaling cascades. The retinoschisin–Na/K-ATPase complex also overlapped with Na/K-ATPase–associated intracellular signaling transducers. Finally, retinoschisin treatment markedly affected Na/K-ATPase localization in *Rs1h*$^{-/Y}$ retinae. From these data, we speculate that retinoschisin deficiency may be a trigger for disease pathogenesis by causing defective control of Na/K-ATPase–mediated signaling and localization in the retina.

RESULTS

Specific interaction of retinoschisin with the β2-subunit of the retinal Na/K-ATPase

Our previous studies revealed that the retinal Na/K-ATPase, composed of subunits α3 (ATP1A3) and β2 (ATP1B2), is required for anchorage of retinoschisin to the plasma membrane (Friedrich *et al.*, 2011). We now aimed to further delineate the interaction between retinoschisin and the Na/K-ATPase.

We tested retinoschisin binding to Hek293 cells heterologously expressing different Na/K-ATPase α-subunit isoforms in combination with different β-subunit isoforms (α1-β1, α1-β2, α1-β3, α2-β1, α2-β2, α2-β3, α3-β1, α3-β2, or α3-β3). We addressed membrane transport of all coexpressed subunits via Western blot of isolated cell surface proteins (Supplemental Figure S1A), fluorescence-activated cell sorting (FACS; Supplemental Figure S2), and on-cell Western analyses (Supplemental Figure S3). Our data reveal that all coexpressed α- and β-subunit isoform combinations are transported to the membrane (Supplemental Figures S1–S3). Efficient retinoschisin binding (Figure 1A) was found with all Hek293 cells heterologously expressing β2, independent of the coexpressed α-subunit. Quantification of the binding efficiency showed increased retinoschisin binding of α1-β2–expressing Hek293 cells (1.50 ± 0.33 compared with α3-β2 in three independent replications, $p = 0.12$). Our analyses do not reveal whether this increase is caused by increased membrane expression or increased retinoschisin affinity of α1-β2 Na/K-ATPases. No retinoschisin binding was detected in Hek293 cells heterologously expressing β1 or β3 in combination with any of the α-subunit isoforms.

To specify the retinoschisin interaction domain of ATP1B2, we generated chimeras of ATP1B1 and ATP1B2 consisting of the inner-membrane and transmembrane domains of ATP1B2 (aa 1–79) fused to the outer domain of ATP1B1 (aa 74–303; ATP1B1-OD), as well as constructs composed of the inner-membrane and transmembrane domains of ATP1B1 (aa 1–71) and the outer domain of ATP1B2 (aa 77–291; ATP1B2-OD). ATP1B1-OD was exported to the plasma membrane, as revealed by anti-β1 Western blot analyses of isolated cell surface proteins (Supplemental Figure S1B). However, in contrast to the regular β1-subunit, the construct containing the outer domain of ATP1B1 was only weakly recognized in FACS (Supplemental Figure S2) and on-cell Western analyses (Supplemental Figure S3). This could be explained by altered outer domain folding of the chimeric construct compared with regular ATP1B1. Proteins were not denatured before subjection to antibodies in FACS or on-cell Western analyses. The epitope recognized by the anti-β1 antibody could thus be less accessible in the native ATP1B1-OD constructs but take on an open configuration after denaturation for Western blot analysis, a discrepancy observed for many other proteins (e.g., Laman *et al.*, 1993; McKnight *et al.*, 1996).

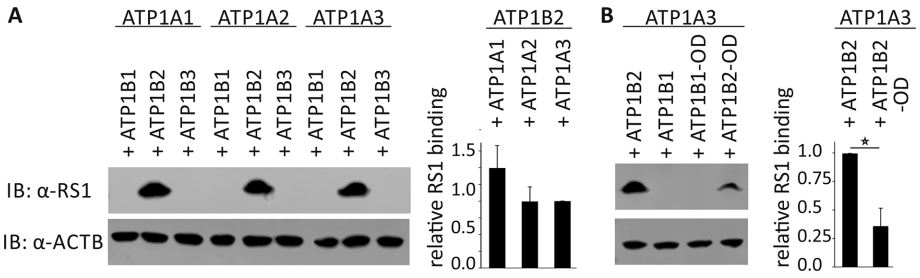

FIGURE 1: Binding of retinoschisin to Na/K-ATPases of different subunit compositions. (A) Hek293 cells were transfected with expression vectors for ATP1A1, ATP1A2, or ATP1A3 in combination with expression vectors for ATP1B1, ATP1B2, or ATP1B3. (B) Hek293 cells were transfected with an expression vector for ATP1A3 in combination with an expression vector for ATP1B2 or ATP1B1 or expression vectors for ATP1B1-OD (outer domain of ATP1B1 fused to inner and transmembrane domains of ATP1B2) or ATP1B2-OD (outer domain of ATP1B2 fused to inner and transmembrane domains of ATP1B1). After transfection, Hek293 cells were incubated for 60 min with retinoschisin-containing supernatant of cells stably transfected with a retinoschisin expression vector. Cells were then centrifuged and intensively washed. Retinoschisin binding was assessed by subjecting cell pellets to Western blot analyses with antibodies against retinoschisin. The Actb immunoblot was performed as loading control. Densitometric quantification of retinoschisin binding was based on immunoblot evaluation from three independent experiments. Signals were normalized against Actb and calibrated against binding to ATP1B2-ATP1A3–transfected cells. Data represent mean ± SD. Underlined asterisk marks statistically significant ($p < 0.05$) differences.

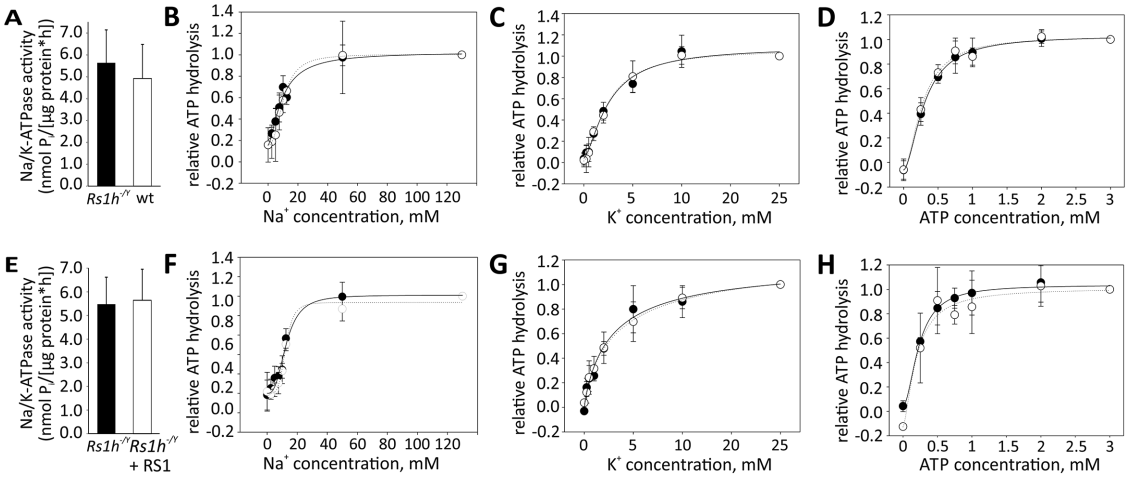

FIGURE 2: Influence of retinoschisin on ATP hydrolysis and substrate affinity of the retinal Na/K-ATPase. (A) Na/K-ATPase–catalyzed (ouabain sensitive) ATP hydrolysis in retinal membranes fractions from each of 11 *Rs1h*$^{-/Y}$ and wild-type (wt) mice. (B–D) Na/K-ATPase–catalyzed ATP hydrolysis in retinal membrane fractions from *Rs1h*$^{-/Y}$ (closed circles) and wild-type (open circles) mice as a function of Na^+ (B, $n = 4$), K^+ (C, $n = 4$), and ATP (D, $n = 3$). (E) Na/K-ATPase–catalyzed (ouabain-sensitive) ATP hydrolysis in each of 11 *Rs1h*$^{-/Y}$ murine retinal membranes fractions preincubated for 30 min with or without recombinant retinoschisin (1 µg/ml). (F–H) Na/K-ATPase–catalyzed ATP hydrolysis in *Rs1h*$^{-/Y}$ retinal membrane fractions preincubated with (open circles) or without (closed circles) retinoschisin as a function of Na^+ (F, $n = 4$), K^+ (G, $n = 4$), and ATP (H, $n = 3$). The maximal enzymatic activity was determined in complete buffer system for each preparation separately. Data are given as mean ± SD. Primary data for ATP hydrolysis with or without ouabain are given in Supplemental Figure S4.

ATP1B2-OD was recognized on the surface of transfected Hek293 cells via all three methodological approaches (Supplemental Figures S1B, S2, and S3). Nevertheless, differences in the FACS signals were obvious when compared with regular ATP1B2 (Supplemental Figure S2), probably also indicating a slight difference in the three-dimensional structure of the outer domain of the chimeric ATP1B2-OD construct compared with regular ATP1B2.

We tested the ability of the chimeric constructs to bind recombinant retinoschisin, which was observed only with ATP1B2-OD (Figure 1B). Nevertheless, binding efficiency of retinoschisin to ATP1B2-OD was strongly reduced compared with ATP1B2 (0.36 ± 0.16, $p = 0.02$, in three independent assays), which could be an effect of a slightly altered outer domain structure of ATP1B2-OD, as suggested by the FACS signals.

Influence of retinoschisin on active ion transport of the retinal Na/K-ATPase

To characterize the functional effect of retinoschisin binding on the retinal Na/K-ATPase, we investigated whether retinoschisin binding affects the active ion pump activity of the Na/K-ATPase.

We investigated Na/K-ATPase catalyzed (ouabain-sensitive) ATP hydrolysis in retinal membrane fractions of retinoschisin-deficient and wild-type mice. Previous analyses showed that retinoschisin deficiency in *Rs1h*$^{-/Y}$ mice had no effect on protein levels of Atp1a3 and Atp1b2 in the murine retina (Friedrich *et al.*, 2011). Now, our enzymatic assay revealed no significant differences ($P = 0.287$) in enzymatic activity between 11 retinal membrane fractions from *Rs1h*$^{-/Y}$ and wild-type mice (Figure 2A). Specific activities were 4.9 ± 1.6 nmol phosphate (Pi) per hour and microgram protein (nmol Pi/µg protein h) for wild-type mice and 5.6 nmol ± 1.5 nmol Pi/(µg protein h) for *Rs1h*$^{-/Y}$ mice, in line with published Na/K-ATPase activities in enriched membrane fractions (e.g., Delamere and King, 1992).

Binding of FDXY2 to the Na/K-ATPase was reported to influence its substrate affinity but not its activity under optimal test conditions (Jones *et al.*, 2005). We thus explored the influence of retinoschisin on substrate affinity of the retinal Na/K-ATPase by testing the affinities for Na^+, K^+, and ATP via the ouabain-sensitive ATP hydrolysis assay in retinal membrane fractions (Jones *et al.*, 2005). Comparing Na/K-ATPase activities of membrane fractions from murine *Rs1h*$^{-/Y}$ retinae to those from wild-type retinae, we observed no significant differences in substrate affinities for Na^+ (Figure 2B), K^+ (Figure 2C), and ATP (Figure 2D). The corresponding Michaelis–Menten constants for Na^+, K^+, and ATP were derived from the Michaelis–Menten equation and reveal no statistically significant differences (Table 1).

In addition, we investigated the direct effect of externally added retinoschisin on the retinal Na/K-ATPase activity. Membrane fractions from each of 11 murine *Rs1h*$^{-/Y}$ retinae were incubated for 30 min with or without recombinant retinoschisin before performing the ouabain-sensitive ATP hydrolysis assay. Retinoschisin treatment did not affect specific Na/K-ATPase activities ($p = 0.76$; 5.6 ± 1.3 nmol Pi/(µg protein h) with retinoschisin and 5.5 ± 1.1 nmol Pi/(µg protein

Michaelis–Menten constant (mM)	*Rs1h*$^{-/Y}$	Wild type	*p*
K_m (Na^+)	10.48 ± 2.79	10.53 ± 2.40	0.979
K_m (K^+)	2.35 ± 0.37	2.33 ± 0.35	0.925
K_m (ATP)	0.30 ± 0.07	0.27 ± 0.05	0.573
	Rs1h$^{-/Y}$ control	*Rs1h*$^{-/Y}$ + RS1	*p*
K_m (Na^+)	12.32 ± 0.42	12.17 ± 0.60	0.698
K_m (K^+)	2.20 ± 0.16	2.20 ± 0.45	1.000
K_m (ATP)	0.29 ± 0.06	0.29 ± 0.06	0.956

TABLE 1: Michaelis–Menten constant for retinal Na/K-ATPase from *Rs1h*$^{-/Y}$ and wild-type mice, as well as for retinal Na/K-ATPase from *Rs1h*$^{-/Y}$ mice incubated with or without recombinant retinoschisin (RS1).

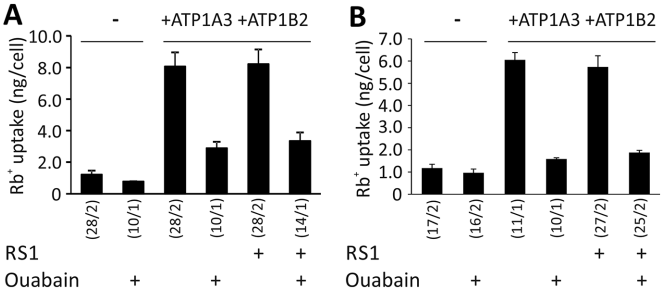

FIGURE 3: Influence of retinoschisin on active ion pump function of the retinal Na/K-ATPase heterologously expressed in *X. laevis* oocytes. Oocytes were injected with cRNAs for human ATP1A3 and ATP1B2 and incubated for 3 d. Rb^+ uptake was determined with or without ouabain (10 mM) at pH 5.5 in a solution containing 5 mM Rb^+. (A) Oocytes were preincubated for 1 h with or without 1 µg/ml retinoschisin. (B) Oocytes were preincubated for 1 h with or without 8 µg/ml retinoschisin. The number of replicates (number of cells/number of independent cell batches) is given in brackets. Data are presented as mean ± SEM.

h) without retinoschisin; Figure 2E), as well as affinities for Na^+ (Figure 2F), K^+ (Figure 2G), and ATP (Figure 2H). Michaelis–Menten constants are given in Table 1.

Finally, we assessed the effect of retinoschisin on the human retinal Na/K-ATPase (ATP1A3 and ATP1B2) heterologously expressed in *Xenopus laevis* oocytes. As a common strategy to eliminate the contribution of endogenous Na/K-ATPases (Cougnon *et al.*, 1998; Koenderink *et al.*, 2000; Dürr *et al.*, 2013; Spiller and Friedrich, 2014), we used an ouabain-resistant ATP1A3 protein with an half-maximal inhibitory concentration (IC_{50}) in the millimolar range (Price and Lingrel, 1988; Dürr *et al.*, 2013). The retinal Na/K-ATPase ion pump activity was assessed by measuring the amount of rubidium cation (Rb^+) transported into the cells, which are recognized as congeners of K^+ by the Na/K-ATPase (Post *et al.*, 1972; Beauge and Glynn, 1979). Intracellular Rb^+ was determined via atomic absorption spectrophotometry (Dürr *et al.*, 2013). All assays were conducted in the presence of 10 µM ouabain to inhibit endogenous Na/K-ATPase activity. On heterologous expression of the retinal Na/K-ATPase, Rb^+ uptake by oocytes increased approximately sixfold compared with untransfected oocytes (Figure 3). The average uptake was 7 ng Rb^+ per transfected oocyte in 3 min (corresponding to 7899 nC), which is in line with published results for Na/K-ATPase activity in transfected oocytes (Dürr *et al.*, 2013). Ouabain at 10 mM led to an inhibition of the heterologously expressed Na/K-ATPase by ~80% (Figure 3). The addition of 1 µg/ml retinoschisin had no effect on ion-pumping activity of the Na/K-ATPase (Figure 3A). An increase to 8 µg/ml retinoschisin also revealed no effects (Figure 3B).

Effect of retinoschisin binding on Src activation

We recently showed that treatment with recombinant retinoschisin decreases the strong endogenous ERK pathway activation in retinoschisin-deficient retinal cell lines and *Rs1h*$^{-/Y}$ retinae (Plössl *et al.*, 2017). Activation of the tyrosine-protein kinase Src was described as one exemplary possibility to regulate ERK signaling by Na/K-ATPases (Haas *et al.*, 2002; Tian *et al.*, 2006; Quintas *et al.*, 2010; Reinhard *et al.*, 2013; Banerjee *et al.*, 2015; Yosef *et al.*, 2016). We thus investigated whether retinoschisin affects Src activation by following Src phosphorylation on tyrosine 416 and determining the effect of the Src kinase inhibitor 4-amino-5-[chlorophenyl]-7-[*t*-butyl] pyrazolo[3,4-*d*]pyrimidine (PP2) on Erk1/2 activation.

Murine *Rs1h*$^{-/Y}$ retinal explants were treated for 10 and 30 min with recombinant retinoschisin, which was purified from supernatant of Hek293 cells heterologously expressing Myc-tagged retinoschisin. This was compared with explants treated with the same volume of control protein eluate (prepared from supernatant of empty vector–transfected cells). As a control, we also tested the effect of the purified XLRS-associated retinoschisin mutant RS1-C59S (NM_000330.3(RS1):c.175T>A [p.Cys59Ser]; https://databases.lovd.nl/shared/variants/RS1/unique?search_var_status=%3D%22Marked%22%7C%3D%22Public%22). A fourth batch of explants was incubated with control protein plus PP2. As shown in Figure 4A, 10 min of retinoschisin treatment slightly reduced Src phosphorylation (86.8 ± 2.9%) compared with control treatment but with a statistically highly significant difference between retinoschisin and control treatment ($p = 4.9 \times 10^{-4}$). RS1-C59S did not cause down-regulation of Src activity (110.9 ± 23.8% compared with control). After 30 min of treatment, an influence of retinoschisin on Src phosphorylation was no longer detectable. PP2 treatment resulted in almost complete dephosphorylation of Src (pSrc level ~25% at 10 min and 10% at 30 min). A change in total Src levels by retinoschisin or PP2 was not observed (Figure 4A), indicating that expression or stability of Src was not affected by the various treatments.

We previously reported that 30 min of retinoschisin treatment reduced Erk1/2 activation by ~30% (68.7 ± 18.2% compared with control; Plössl *et al.*, 2017). We show now that the inhibition of Src by PP2 leads to a strong and statistically highly significant down-regulation of Erk1/2 phosphorylation after 30 min of incubation (50.0 ± 11.8%; $p = 6.8 \times 10^{-4}$ compared with control protein–treated samples; Figure 4B). Total Erk1/2 levels were not affected by PP2, excluding an effect on expression or stability of Erk1/2.

Effect of retinoschisin on PI3K/Akt signaling

In specific cell types, the Na/K-ATPase was capable of inducing PI3K/Akt signaling (Aperia *et al.*, 2016). Therefore we investigated the influence of retinoschisin on PI3K/Akt signaling by following phosphorylation of Akt on serine 473 in *Rs1h*$^{-/Y}$ murine retinal explants (Figure 5). Explants treated with retinoschisin, RS1-C59S, or control protein showed no differences in Akt activation at 10 or 30 min of incubation. The different treatments also had no effect on total Akt protein levels in murine retinal explants (Figure 5).

Effect of retinoschisin on Ca^{2+} signaling

In addition to ERK and PI3K/Akt signaling, the Na/K-ATPase was reported to influence Ca^{2+} signaling (Aperia *et al.*, 2016). We examined an effect of retinoschisin on Ca^{2+} signaling by following phosphorylation of Ca^{2+}/calmodulin-dependent protein kinase II (Camk2) on threonine 286 in *Rs1h*$^{-/Y}$ murine retinal explants (Figure 6A).

Camk2 activation was not affected by 10 min of treatment with retinoschisin or RS1-C59S. However, we observed a strong effect of retinoschisin on Camk2 activation in *Rs1h*$^{-/Y}$ murine retinal explants after 30 min of incubation time. Phosphorylated Camk2 levels were significantly down-regulated in retinoschisin-treated explants (61.4 ± 15.5%) compared with control protein treated explants ($p = 0.008$) or explants treated with RS1-C59S (107.2 ± 32.3%, $p = 0.045$; Figure 6A). Total Camk2 levels were not affected by retinoschisin, RS1-C59S, or PP2 treatment (Figure 6A).

Because Ca^{2+} signaling can also influence ERK activation (e.g., Illario *et al.*, 2003; Rusciano *et al.*, 2010), we tested the effect of Ca^{2+} signaling inhibitor 2-aminoethoxydiphenyl borate (2-APB; inhibits inositol 1,4,5-trisphosphate receptor function) on phosphorylation of Erk1/2 (Figure 6B). Of interest, treatment with 2-APB led to a strong decrease in phosphorylated Erk1/2 levels after 30 min of incubation (36.0 ± 9.6%, $p = 0.003$), whereas total Erk1/2 levels were not affected.

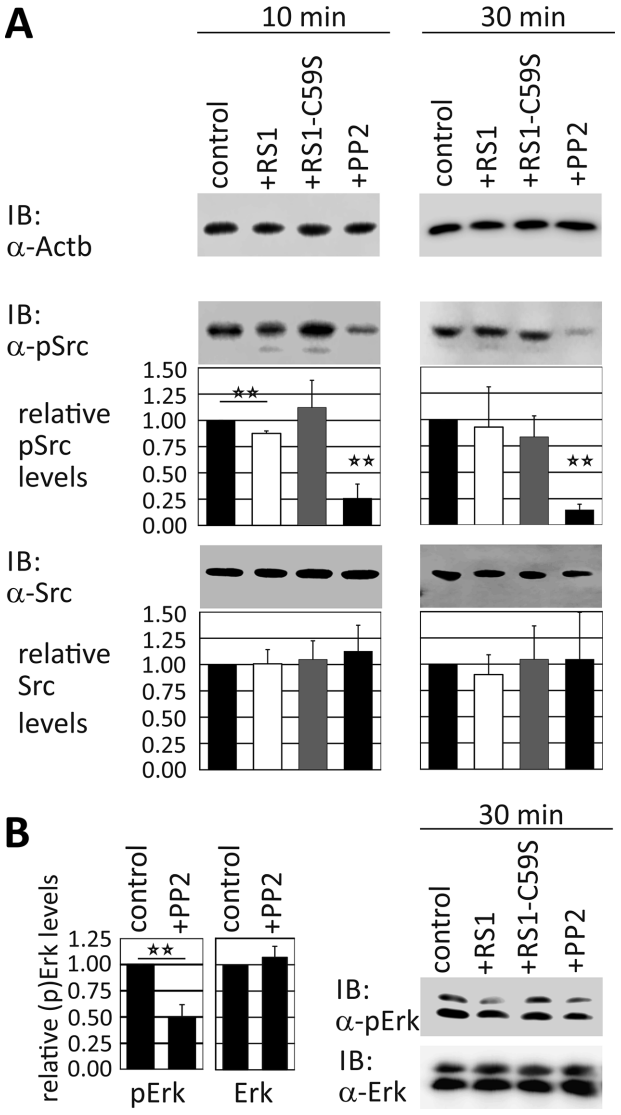

FIGURE 4: Involvement of Src on retinoschisin-induced Erk deactivation. Murine *Rs1h*$^{-/Y}$ retinal explants were treated for 10 and 30 min with retinoschisin, RS1-C59S, or control protein. Additional experiments were performed in the presence of Src inhibitor PP2 (5×10^{-5} M). After treatment, the cells were subjected to Western blot analyses with antibodies against (A) phosphorylated Src (pSrc) and total Src, as well as against (B) phosphorylated Erk1 and Erk2 (pErk1/2) and total Erk1 and Erk2 (Erk1/2). Actb staining served as control. Densitometric quantification was performed with immunoblots from five independent experiments. Signals were normalized against Actb and calibrated against the control. Data represent mean ± SD. Underlined double asterisks denote statistically highly significant ($p < 0.01$) differences between results of two different treatments; double asterisks on the PP2-treated sample denotes statistically highly significant difference ($p < 0.01$) from control treatment.

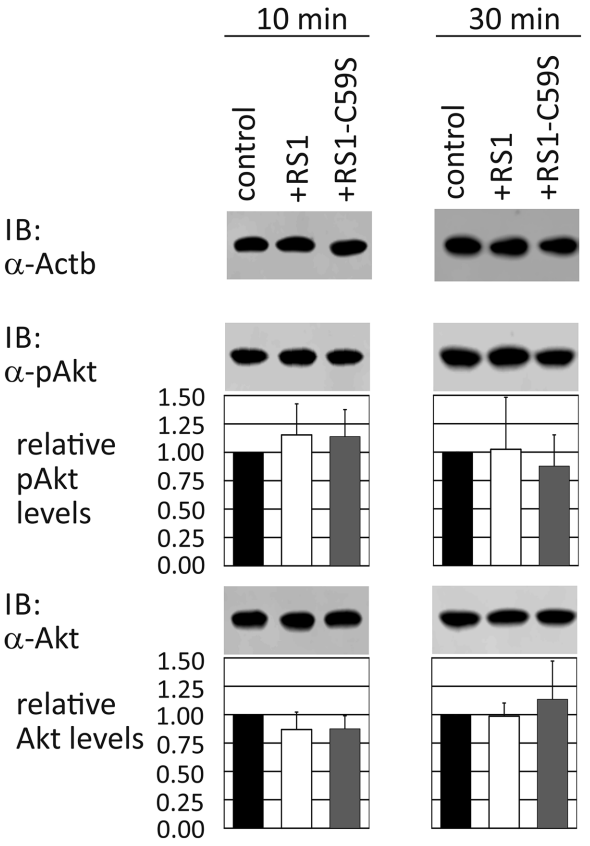

FIGURE 5: Effect of retinoschisin on PI3K/Akt signaling. *Rs1h*$^{-/Y}$ retinal explants were treated for 10 and 30 min with retinoschisin, RS1-C59S, or control protein. After treatment, the cells were subjected to Western blot analyses with antibodies against phosphorylated Akt (pAkt), total Akt, and Actb as control. Densitometric quantification was performed with immunoblots from five independent experiments. Signals for pAkt and Akt were normalized against Actb and calibrated against the control.

Colocalization of the retinoschisin–Na/K-ATPase complexes with scaffolding proteins and intracellular signal transducers

Scaffolding proteins such as ankyrin or caveolin that anchor Na/K-ATPases to specific membrane microdomains, as well as a close association or proximity to intracellular signal transmitters, play an important role in the regulation of Na/K-ATPase signaling (Wang *et al.*, 2004; Liang *et al.*, 2007; Liu *et al.*, 2008; Quintas *et al.*, 2010; Bai *et al.*, 2016). We thus addressed colocalization of the retinal Na/K-ATPase with retinoschisin, scaffolding proteins, and intracellular Na/K-ATPase–associated signal transmitters in 10-d-old murine wild-type retinae via immunohistochemistry.

As documented before (Friedrich *et al.*, 2011), strong retinoschisin signals were found in photoreceptor inner segments. Weak retinoschisin staining was also observed in the outer plexiform layer and outer nuclear layer (Supplemental Figure S5). A similar distribution was obtained for retinal Na/K-ATPase subunits Atp1a3 (Supplemental Figure S5A) and Atp1b2 (Supplemental Figure S5B). A focus on the retinoschisin-containing retinal layers (inner segments, outer nuclear layer, and outer plexiform layer) revealed colocalization between retinoschisin and Na/K-ATPase subunits Atp1a3 (Figure 7A) and Atp1b2 (Figure 7B). Pearson's coefficients were >0.5 and overlap coefficients >0.9 (Supplemental Table S1).

In several tissues, Na/K-ATPase complexes are concentrated in caveolae by caveolin-1, a process affecting Na/K-ATPase–mediated signaling (Wang *et al.*, 2004; Liang *et al.*, 2007; Quintas *et al.*, 2010; Bai *et al.*, 2016). Immunohistochemistry depicted strong caveolin-1 signals from outer to inner plexiform layers and in a horizontal line between inner segments and outer nuclear layer (Supplemental Figure S5C). In addition, weak signals were obtained in the inner segments and outer nuclear layer. This pattern is consistent with

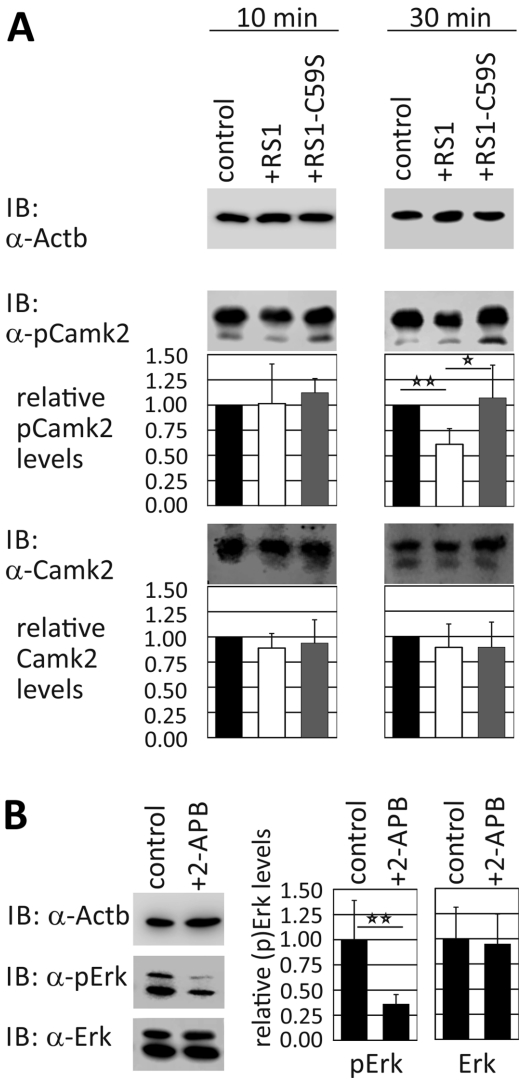

FIGURE 6: Effect of retinoschisin on Ca^{2+} signaling. (A) *Rs1h*$^{-/Y}$ retinal explants were treated for 10 and 30 min with retinoschisin, RS1-C59S, or control protein. After treatment, the cells were subjected to Western blot analyses with antibodies against phosphorylated Camk2 (pCamk2), total Camk2, and Actb as control. Densitometric quantification was performed with immunoblots from five independent experiments. Signals for pCamk2 and Camk2 were normalized against Actb and calibrated against the control. Data represent mean ± SD. (B) *Rs1h*$^{-/Y}$ retinal explants were treated for 30 min with Ca^{2+} signaling (IP3 receptor) inhibitor 2-APB. To assess an effect of the Ca^{2+} pathway on Erk1/2 activation, the cells were subjected to Western blot analyses with antibodies against phosphorylated Erk1 and Erk2 (pErk1/2), total Erk1 and Erk2 (Erk1/2), and Actb as control. Underlined asterisk marks statistically significant ($p < 0.05$) and underlined double asterisks statistically highly significant ($p < 0.01$) differences between results of two different treatments.

previous studies, in which caveolin-1 was expressed predominantly in Müller cells (Li *et al.*, 2012; Gu *et al.*, 2014) but also weakly in photoreceptor inner segments (Berta *et al.*, 2011; Li *et al.*, 2012). Focusing on the region from inner segments to outer plexiform layer, we observed an overlap between retinoschisin and caveolin-1 staining in inner segments, outer nuclear layer, and inner plexiform layer but not with caveolin-1 signals from Müller cells (the horizontal line between inner segments and outer nuclear layer; Figure 7C). This makes the application of Pearson's coefficients for quantification of colocalization unsuitable (Dunn *et al.*, 2011). Nevertheless, overlap coefficients had high values (~0.9; Supplemental Table S1). As previously shown (Berta *et al.*, 2011), the intracellular signal transmitter Src had a very similar staining pattern as caveolin-1, with additional signals in the outer segments (Supplemental Figure S5D and Figure 7D). Overlap coefficients of ~0.9 were obtained (Supplemental Table S1).

In several vertebrate retinae, the Na/K-ATPase is restricted to the inner segment of photoreceptors by ankyrin-B (Kizhatil *et al.*, 2009). Concentrated by ankyrin-B, the Na/K-ATPase formed signaling microdomains with the inositol-3-phosphate (IP3) receptor (Mohler *et al.*, 2005; Liu *et al.*, 2008), an endoplasmic reticulum membrane–localized Ca^{2+} channel (Miyakawa-Naito *et al.*, 2003; Yuan *et al.*, 2005), in several cell types. Colocalization of ankyrin-B and the retinal Na/K-ATPase in murine and other vertebrate retinae has been demonstrated (Kizhatil *et al.*, 2009). Our immunohistochemical analyses revealed a strong immunohistochemical IP3 receptor signal in inner segments, inner nuclear layer, and plexiform layers and a weak signal in the outer nuclear layer (Supplemental Figure S5E), in agreement with previous results (Day *et al.*, 1993). Retinoschisin and the IP3 receptor partially overlapped in inner segments, outer nuclear layer, and outer plexiform layer (Figure 7E), with Pearson's values of ~0.5 and overlap coefficients of ~0.9 (Supplemental Table S1). Phospholipase C (Plc), a signal transmitter possibly involved in Na/K-ATPase–mediated Ca^{2+} signaling (Miyakawa-Naito *et al.*, 2003; Yuan *et al.*, 2005), had a similar distribution as the IP3 receptor over the entire retina but with signals extending to outer segments (Supplemental Figure S5F). Immunohistochemistry revealed a partial overlap with retinoschisin (Figure 7E). Quantification resulted in overlap coefficients of ~0.9 but low Pearson's coefficients (~0.2; Supplemental Table S1).

Effect of retinoschisin on Na/K-ATPase localization

Retinal cryosections from *Rs1h*$^{-/Y}$ eyes showed increasing mislocalization of the Na/K-ATPase during retinal development (Friedrich *et al.*, 2011). More precisely, Atp1a3 and Atp1b2 immunoreactivity was reduced in the inner segments of photoreceptors and increased in the outer nuclear layer (Friedrich *et al.*, 2011), as specifically evident in retinae at postnatal day 18.

We now sought to assess whether retinoschisin directly affects retinal Na/K-ATPase localization. Thus we treated *Rs1h*$^{-/Y}$ retinal explants at postnatal day 18 with recombinant retinoschisin, RS1-C59S, and control protein. After 1 wk of incubation, we followed retinoschisin binding and Na/K-ATPase localization via immunohistochemistry against retinoschisin and Atp1a3 (Figure 8). Explants treated with RS1-C59S or control protein showed no retinoschisin signal and exhibited almost even distribution of Atp1a3 in inner segments and outer nuclear layer of photoreceptors (Figure 8, A and C). Of note, explants treated with recombinant retinoschisin had a strong clustering of the Na/K-ATPase and retinoschisin in the photoreceptor inner segments, accompanied by reduced Na/K-ATPase signals in the inner nuclear layer (Figure 8B).

DISCUSSION

In this study, we were interested in evaluating the functional effect of retinoschisin on its binding partner in the retina, the retinal Na/K-ATPase. Our data reveal a specific interaction of retinoschisin with the outer domain of Na/K-ATPase subunit β2. Investigations into the ion pump activity and substrate affinity of Na/K-ATPase failed to detect a regulatory effect of retinoschisin on these functions. In addressing the signal-transducing aspect of the Na/K-ATPase, we

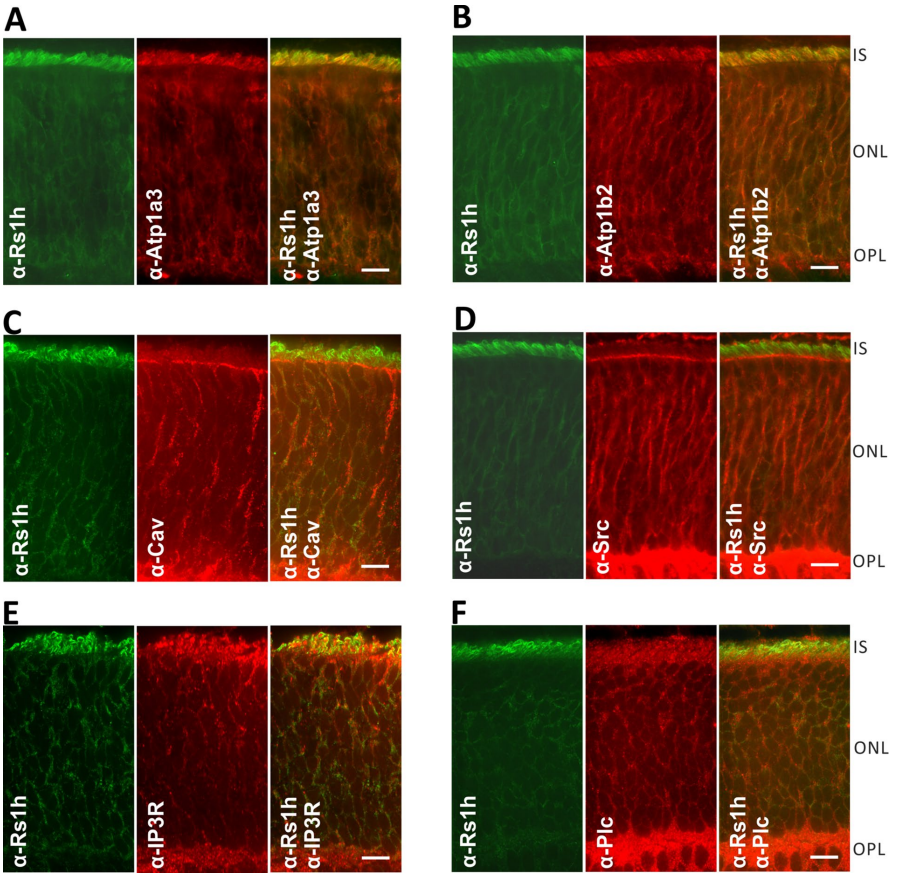

FIGURE 7: Colocalization of retinoschisin, the Na/K-ATPase, and Na/K-ATPase–associated signaling mediators in murine retinae. Retinal cryosections from wild-type mice at postnatal day 10 were labeled with antibodies against retinoschisin (Rs1h) and Atp1a3 (A), Atp1b2 (B), caveolin (cav; C), Src (D), Plc (E), or the IP3 receptor (IP3R; F). Confocal microscope images were taken under 100× magnification. Retinal layers are indicated on the right; IS, inner segments; ONL, outer nuclear layer; OPL, outer plexiform layer. Scale bar, 10 μm.

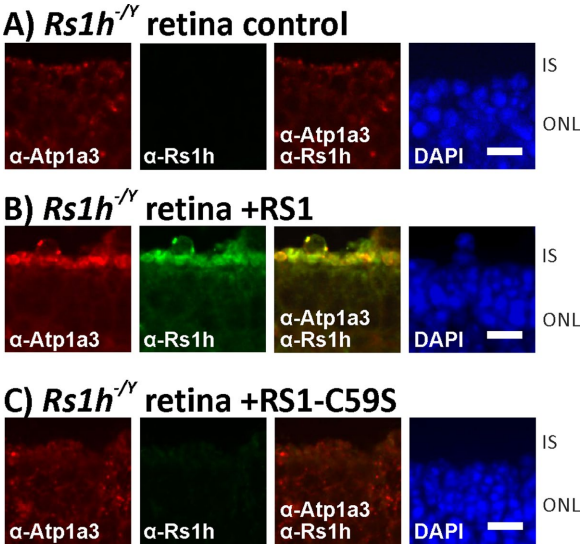

FIGURE 8: Effect of retinoschisin Na/K-ATPase localization. *Rs1h*$^{-/Y}$ retinal explants harvested at postnatal day 18 were cultured for 1 wk in medium containing retinoschisin, RS1-C59S, or control protein. After washing and embedding, cryosections of these explants were subjected to staining for nuclei, Atp1a3, and retinoschisin. IS, inner segments; ONL, outer nuclear layer. Scale bar, 10 μm.

found that applying recombinant retinoschisin to *Rs1h*$^{-/Y}$ murine retinal explants modulated Src activation as well as Ca^{2+} signaling, in addition to the known deactivation of the Erk pathway. As expected, the XLRS-associated mutant RS1-C59S failed to reveal an effect on intracellular signaling. Immunohistochemistry demonstrated a good colocalization of retinoschisin with the retinal Na/K-ATPase and an overlap of the retinoschisin–Na/K-ATPase complex with well-described mediators of Na/K-ATPase signaling, including caveolin, Src, Plc, and the IP3 receptor. Finally, recombinant retinoschisin affected localization of the Na/K-ATPase in *Rs1h*$^{-/Y}$ murine retinal explants. Together, these findings suggest the existence of a retinoschisin–Na/K-ATPase signalosome modulating intracellular signaling pathways in the retina.

The activity of Na/K-ATPases is subjected to a strict regulation at several levels, among which is via an interaction with Na/K-ATPase–binding proteins, such as members of the FXYD family (Geering, 2006), caveolin (Liang *et al.*, 2007; Quintas *et al.*, 2010; Yosef *et al.*, 2016), ankyrin, actin, and adducin (Therien and Blostein, 2000). Similar to these proteins, retinoschisin may also act as a newly recognized modulator of Na/K-ATPase activity.

Our experiments show that retinoschisin binding specifically requires the extracellular domain of the β2-subunit, whereas the α-subunit is exchangeable. This result is in line with data on the crystal structure of the Na/K-ATPase, for which a huge extracellular domain of the β-subunit was described to almost completely cover the extracellular parts of the α-subunit (Morth *et al.*, 2007).

The α-subunit of Na/K-ATPases is the catalytic subunit, mediating active ion transport and steroid hormone–induced signaling, whereas the accessory β2-subunit controls membrane integration, stability, and activity of the α-subunit (reviewed by Geering, 2008). Binding of retinoschisin to the β2-subunit could alter the modulatory effect of β2 on the activity of the α-subunit and thus affect ion transport or signaling. We could not detect an influence of retinoschisin on active ion pump function or substrate affinity of the retinal Na/K-ATPase. However, our results suggest an influence of retinoschisin on Na/K-ATPase–mediated intracellular signaling cascades.

Recombinant retinoschisin reduced internal activation of nonreceptor tyrosine kinase Src, an initial signal transducer of Na/K-ATPase–mediated signaling (Tian *et al.*, 2006; Reinhard *et al.*, 2013; Banerjee *et al.*, 2015; Yosef *et al.*, 2016), in retinoschisin-deficient retinal explants. Studies have reported that ERK signaling by the Na/K-ATPase is induced via initial activation of Src (e.g., Haas *et al.*, 2002; Quintas *et al.*, 2010). Consistent with this, recombinant retinoschisin reduced internal Src activation in retinoschisin-deficient retinal explants before Erk1/2 activation. Furthermore, the application of Src kinase inhibitor PP2 inhibited Erk1/2 phosphorylation in our retinal model system. Thus our data are consistent with data on timeline and interdependence of Src and MAP kinase activation

after external Na/K-ATPase stimulation (Haas *et al.*, 2002). Nevertheless, with only 14% reduction, effects of retinoschisin on Src phosphorylation were rather small. This may be explained by the specific localization of Src in the murine retina. Immunohistochemical stainings revealed that Src and retinoschisin are expressed in the photoreceptor inner segments, the outer nuclear layer, and the outer plexiform layer. However, in contrast to retinoschisin, there is a strong enrichment of Src in the inner nuclear and inner plexiform layers. This Src pool is most likely not subjected to regulation by the retinoschisin–Na/K-ATPase complex. Another explanation for the weak effect of retinoschisin on Src is provided by a recent study showing that the α3-subunit isoform, which is the predominant α-isoform in photoreceptor cells (85% α3 vs. 15% α1; Schneider and Kraig, 1990), is incapable of inducing Src activation (Madan *et al.*, 2017). Only Na/K-ATPase complexes containing the α1-isoform of the Na/K-ATPase could thus affect Src activation in our model system. Finally, the question arises how the temporary effect of retinoschisin on Src inhibition can relate to the chronic in vivo situation, characterized by a constant hyperactivation of ERK signaling in the XLRS mouse (Gehrig *et al.*, 2007). Of interest, α3–Na/K-ATPases were reported to induce ERK signaling in a Src-independent but so-far-undetermined way (Madan *et al.*, 2017). The observed chronic increase in ERK activation could thus be a consequence of constant misregulation of the predominant α3–β2 Na/K-ATPase isoforms by retinoschisin deficiency.

In addition to ERK signaling, Na/K-ATPase is known to regulate PI3K/Akt and Ca^{2+} signaling (Aperia *et al.*, 2016). Our findings revealed no influence of retinoschisin on PI3K/Akt signaling but demonstrated an inhibiting effect on Ca^{2+} signaling: exposing murine *Rs1h*$^{-/Y}$ retinae to retinoschisin caused strong down-regulation of phosphorylated Camk2, a marker for activated Ca^{2+} signaling (Illario *et al.*, 2003). Inhibition of the IP3 receptor–induced Ca^{2+} signaling pathway by 2-APB resulted in a strong Erk1/2 deactivation, demonstrating involvement of Ca^{2+} signaling in the regulation of the ERK pathway, as observed in other cell types (Illario *et al.*, 2003; Rusciano *et al.*, 2010). One can thus speculate about a long-term effect of the retinoschisin–Na/K-ATPase complex on ERK signaling via its regulation of Ca^{+} signaling.

The Na/K-ATPase serves as a docking station for a variety of protein interaction partners (Reinhard *et al.*, 2013). In several tissues, the Na/K-ATPase is concentrated in caveolae by caveolin-1, a process that significantly influences Na/K-ATPase–mediated signaling (Wang *et al.*, 2004; Liang *et al.*, 2007; Quintas *et al.*, 2010; Bai *et al.*, 2016). Our immunohistochemical analyses revealed an overlap of the retinoschisin–Na/K-ATPase complex with caveolin-1 in murine photoreceptors but no specific enrichment of caveolin-1 along with the retinal Na/K-ATPase in plasma membrane of inner segments as observed for the scaffolding protein ankyrin-B (Kizhatil *et al.*, 2009).

Although it is widely accepted that the tyrosine-protein kinase Src is one possible initial signal transmitter in Na/K-ATPase–mediated signaling, the mechanism is under debate. Whereas some studies suggest a direct interaction between the Na/K-ATPase and Src (Wang *et al.*, 2004; Tian *et al.*, 2006; Banerjee *et al.*, 2015), several others reported evidence against a direct interaction between the Na/K-ATPase and Src (Weigand *et al.*, 2012; Clifford and Kaplan, 2013; Gable *et al.*, 2014; Yosef *et al.*, 2016). Our immunohistochemical data argue against an enrichment of Src along with the Na/K-ATPase–retinoschisin complex at the photoreceptor membrane but show a partial overlap of both proteins in photoreceptors inner segments, suggesting that Src could be affected by Na/K-ATPase signaling in substructures of the retina.

In several vertebrate retinae, the Na/K-ATPase is restricted to the inner segment of photoreceptors by ankyrin-B (Kizhatil *et al.*, 2009). Concentrated by ankyrin-B, the IP3 receptor and the Na/K-ATPase build a functional signaling complex that links plasma membrane to intracellular Ca^{2+} stores from the endoplasmic reticulum, and involvement of intracellular signal transducer Plc in this complex is under discussion (Aizman and Aperia, 2003; Miyakawa-Naito *et al.*, 2003; Yuan *et al.*, 2005; Liu *et al.*, 2008). Although no specific enrichment of the IP3 receptor and Plc was shown for plasma membrane regions of inner segments in our analyses, the retinoschisin–Na/K-ATPase complex overlapped with the IP3 receptor, as well as with Plc, making a functional contact between the Na/K-ATPase and these signaling constituents arguable.

The assembly of Na/K-ATPase signaling complexes is significantly involved in the induction and regulation of Na/K-ATPase–mediated signaling (Therien and Blostein, 2000; Xie and Askari, 2002; Xie and Cai, 2003; Wang *et al.*, 2004; Yuan *et al.*, 2005; Quintas *et al.*, 2010; Reinhard *et al.*, 2013). We previously showed that retinoschisin deficiency leads to an altered localization of the Na/K-ATPase during retinal development (Friedrich *et al.*, 2011). Our data now reveal a direct modulation of Na/K-ATPase localization in murine *Rs1h*$^{-/Y}$ retinal explants by recombinant retinoschisin. Specifically, retinoschisin treatment of murine *Rs1h*$^{-/Y}$ retinal explants resulted in a concentration of retinoschisin–Na/K-ATPase complexes at the photoreceptor inner segments, producing a Na/K-ATPase distribution comparable to that in wild-type retinae (Friedrich *et al.*, 2011). These data indicate that retinoschisin binding is necessary to establish the proper localization of the Na/K-ATPase in the retina. It might also be reasonable to speculate about a role of retinoschisin in the correct assembly of retinal Na/K-ATPase signaling complexes and thus the regulation of Na/K-ATPase signaling.

Several studies have documented a major role for MAP kinase and Ca^{2+} dysregulation in the pathogenesis of neuronal degenerative diseases such as Parkinson disease (Cali *et al.*, 2014; Wang *et al.*, 2014), Alzheimer disease (Gartner *et al.*, 1999; Arendt *et al.*, 2000; Cali *et al.*, 2013), and amyotrophic lateral sclerosis (Holasek *et al.*, 2005; Cali *et al.*, 2013). The contribution of MAP kinase and Ca^{2+} signaling to disease can be explained by their involvement in the regulation of cellular processes such as degeneration, adhesion, proliferation, differentiation, and development (Kolkova *et al.*, 2000; Chang and Karin, 2001), processes also involved in the pathogenesis of XLRS (reviewed by Khan *et al.*, 2001; Sikkink *et al.*, 2007; Molday *et al.*, 2012). It would thus be reasonable to assume a major contribution of retinoschisin deficiency–induced signal dysregulation to the characteristic XLRS-associated degenerative processes of the retina. Similar effects on neuronal homeostasis were described for other extracellular interaction partners of Na/K-ATPases, including cardiac glycosides such as ouabain (in low doses; Golden and Martin, 2006; Desfrere *et al.*, 2009) and amyotrophic lateral sclerosis–associated glycoprotein nonmetastatic melanoma protein B (Ono *et al.*, 2016), promoting neuronal survival and differentiation via manipulation of Na/K-ATPase–associated signaling.

Taken together, our results provide broad evidence that retinoschisin binds to the β2-subunit of retinal Na/K-ATPase, leading to the inhibition of Na/K-ATPase–associated signaling cascades and Na/K-ATPase enrichment at photoreceptor inner segments. Retinoschisin and the Na/K-ATPase of the murine retina were found to overlap with intracellular signal tranducers Src, Plc, and the IP3 receptor, well-described mediators of Na/K-ATPase signaling. We suggest that retinoschisin is an important modulator of retinal Na/K-ATPase signaling complexes and any disturbance in Na/K-ATPase–mediated signaling and localization caused by retinoschisin deficiency might

contribute to the initial steps of XLRS pathology. Our findings necessitate a novel look at therapeutic treatment options for this progressive and currently untreatable disease.

MATERIALS AND METHODS

Animal models

The *Rs1h*$^{-/Y}$ mouse was generated as described previously (Weber *et al*., 2002) and kept on a C57BL/6 background. Mice were housed under specific pathogen-free barrier conditions at the Central Animal Facility of the University of Regensburg and maintained under conditions established by the institution for their use, in strict compliance with National Institutes of Health guidelines. Mice were killed 10, 16, or 18 d after birth by decapitation or cervical dislocation.

Cell culture

Hek293 (human embryonic kidney) cells (Invitrogen, Carlsbad, CA) were maintained in DMEM high-glucose containing 10% fetal calf serum (FCS), 100 U/ml penicillin/streptomycin, and 500 µg/ml G418. All media and cell culture supplies were purchased from Life Technologies (Carlsbad, CA). Hek293 cells were grown in a 37°C incubator with a 5% CO_2 environment and subcultured when they reached 90% confluency.

Primary antibodies

Primary antibodies against phospho-Akt (Ser-473; 4060), Akt (pan; 4691), phospho–Src family (Tyr-416; 6943), Src (2123), phospho-p44/42 MAPK (Erk1/2) (Thr-202/Tyr-204; 4370), PLC-γ1 (5690), IP3 receptor 1 (8569), and caveolin-1 (#3267) were obtained from Cell Signaling Technology (Danvers, MA). Primary antibodies against Na/K-ATPase subunits Atp1a3 (MA3-915) and Atp1b2 (PA5-26279) and phospho–CaM kinase II (Thr-286; PA1-14076), as well as CaM kinase II (PA1-14077) were obtained from Thermo Fisher Scientific. The primary actin beta (Actb; A5441) and Erk1/2 (M5670) antibodies were from Sigma-Aldrich (St. Louis, MO). Primary antibodies against Atp1a1 (55187-1-AP), Atp1a2 (16836-1-AP), and Atp1b1 (15192-1-AP) were obtained from Proteintech (Rosemont, IL). The Atp1b3 (H00000483-B01) antibody was from Abnova (Taipei, Taiwan), and pan-cadherin antibody (ab6528) was from Abcam (Cambridge, United Kingdom). All commercial antibodies were used to the manufacturer's recommendations for Western blotting and immunohistochemistry. The RS1 primary antibody (diluted 1:10,000 for Western blot and 1:1000 for immunohistochemistry) was kindly provided by Robert Molday (University of British Columbia, Vancouver, Canada).

Expression constructs

Generation of expression constructs for ATP1A1 (NM_000701.7), ATP1A2 (NM_000702.3), ATP1B1 (NM_001677.3), and ATP1B3 (NM 001679.3) was performed as described in Friedrich *et al*. (2011) but with primers listed in Supplemental Table S1. Expression constructs for ATP1A3 (NM_152296.4) and ATP1B2 (NM_001678.4) were generated as described in Friedrich *et al*. (2011).

Chimeric constructs of ATP1B1 and ATP1B2 were generated as follows. For construct ATP1B1-OD, the outer domain of ATP1B2 (aa 80–291) was replaced by the corresponding amino acids from ATP1B1 (aa 74–304). Inner domain and transmembrane domain from ATP1B2 (aa 1–79) were fused to the outer domain of ATP1B1 using the endogenous *Msc*I restriction site at aa 77–79 of the ATP1B2 subunit.

For construct ATP1B2-OD, the outer domain of ATP1B2 (aa 77–291) was fused to the inner domain of ATP1B1 (aa 1–73) using the endogenous *Msc*I restriction site (aa 77–79) of the ATP1B2 subunit. Primers for amplifying the partial coding sequences of ATP1B1 and ATP1B2 are given in Supplemental Table S1. The coding sequences of all Na/K-ATPase subunits described were ligated into pCEP4 using restriction sites added with the primers.

The ouabain-insensitive pTLN/ATP1A3 construct was kindly provided by Jan B. Koenderink (Department of Pharmacology and Toxicology, Nijmegen University, Netherlands). A ouabain-insensitive pcDNA3/ATP1A3 construct was generated by excising the ATP1A3 coding sequence from the ouabain-insensitive pTLN/ATP1A3 construct via *Hin*dIII and *Eco*RI.

The pTLN/ATP1B2 was generated by excising the ATP1B2 coding sequence from pCEP+ATP1B2 via *Kpn*I and *Xho*I.

Generation of expression constructs for nontagged and Myc-tagged RS1 variants is described in Plössl *et al*. (2017). The RS1 variants include nonmutant RS1 (RS1, NM_000330.3) and the XLRS-associated RS1 mutant (NM_000330.3(RS1):c.175T>A [p.Cys59Ser]), titled RS1-C59S.

RS1 binding to Hek293 cells

Retinoschisin binding to Hek293 cells heterologously transfected with expression constructs for different Na/K-ATPase subunits was assessed at least three times in independent assays as described by Friedrich *et al*. (2011) but with a prolonged incubation time of 1 h.

Isolation of cell surface proteins by using the Pierce Cell Surface Protein Isolation Kit

To evaluate cell surface localization of different Na/K-ATPase subunit isozyme combinations, Hek293 cells were transfected with expression constructs for the different isozyme combinations in a six-well format. At 48 h after transfection, cell surface proteins were biotinylated using the Pierce Cell Surface Protein Isolation Kit (Thermo Fisher Scientific) and purified according to the manufacturer's instructions. Purified membrane proteins were subsequently analyzed by Western blotting.

On-cell Western assay

Cell surface protein expression was additionally analyzed by staining unpermeabilized cells with antibodies against the different Na/K-ATPase subunit isoforms. These "on-cell Western assays" were performed as established by LI-COR Biosciences (Bad Homburg, Germany), with the following modifications: Hek293 cells were grown on poly-L-lysine–coated 12-well plates and transiently transfected with expression constructs for different Na/K-ATPase subunit isozyme combinations. At 48 h after transfection, cells were fixed in ice-cold 4% paraformaldehyde for 10 min at room temperature. Cells were then washed 5 × 5 min with 400 µl of 1× phosphate-buffered saline (PBS) before being incubated in 300 µl of blocking solution (LI-COR Odyssey blocking buffer 1:1 diluted with Tris-buffered saline [TBS]) for 90 min at room temperature with gentle agitation. The blocking solution was removed, and cells were covered in 100 µl of primary antibody diluted 1:250 in blocking solution. The cells were then incubated overnight at 4°C with gentle rocking. After 5 × 5 min washing with 400 µl of 1× TBS–Tween 20 (TBS-T), cells were incubated with secondary antibodies (IRDye 800CW anti-mouse and anti-rabbit secondary antibodies [LI-COR] diluted 1:800 in blocking solution) for 1 h at room temperature. Finally, cells were subjected to another 5 × 5 min washing with 400 µl of 1× TBS-T before plates were patted dry and imaged using a LI-COR Odyssey imager.

Fluorescence-activated cell sorting

Hek293 cells were transiently transfected with expression constructs for different Na/K-ATPase subunit isozyme combinations. At 48 h after transfection, 3×10^5 cells were subjected to antibody staining

for FACS analysis. During the procedure, cells were kept on ice, centrifugation steps were carried out at 4°C, and all solutions used were precooled. After harvesting, cells were washed twice in 300 µl of PBS plus1% FCS (5 min, 300 × *g*, 4°C) and then incubated in primary antibodies against Na/K-ATPase β-subunits ATP1B2, ATP1B2, and ATP1B3 for 25 min. After two washing steps in 300 µl of PBS plus 1% FCS (5 min, 300 × *g*, 4°C), cells were incubated in secondary antibody solution (Alexa Fluor 488–conjugated anti-mouse or anti-rabbit [Thermo Fisher Scientific], 1:100 in PBS plus 1% FCS) for 25 min and subsequently washed again twice. Cell pellets were resuspended in 100 µl of PBS plus 1% FCS and subjected to FACS analysis using a FACSCanto-II flow cytometer run by Diva software, version 7.0 (BD Biosciences, San Jose, CA).

Expression and purification of recombinant RS1 variants

Expression and purification of recombinant RS1 variants was performed as described by Plössl *et al.* (2017), with all described controls for protein purity.

For use as a treatment control, Hek293 cells were transfected with empty pCDNA3.1 expression vector (Invitrogen), and cultivation medium of these cells was subjected to a purification procedure exactly like that for the medium from cells transfected with RS1 variants.

Dialysis of recombinant retinoschisin

Recombinant retinoschisin (100 µl) to be used in ATP hydrolysis assays was dialyzed against the respective ATP hydrolysis test buffers described later (2 × 500 ml) using a Slide-A-Lyzer MINI Dialysis Device, 10K MWCO (Thermo Fisher Scientific), at 4°C overnight. The dialysis buffer was changed after 5 h, and total dialysis time was 18 h.

Analysis of Na/K-ATPase activity in murine retinal membranes

A plasma membrane–enriched fraction was collected from retinae of wild-type and *Rs1h*$^{-/Y}$ mice at postnatal day 16 as described before (Friedrich *et al.*, 2011) and solubilized in the respective Na/K-ATPase buffer system. For testing the effect of recombinant retinoschisin, *Rs1h*$^{-/Y}$ retinal membrane fractions were incubated for 30 min with or without recombinant retinoschisin (1.25 µg/ml) before starting the experiment. ATP hydrolysis reactions were performed at 37°C for 60 min in a buffer system containing 100 mM Tris/HCl, pH 7.4, 120 mM NaCl, 20 mM KCl, 3 mM ATP, and 3 mM $MgCl_2$, with and without 0.1 mM ouabain. Ouabain-sensitive Pi release (Jones *et al.*, 2005) was measured colorimetrically (Howard and Ridley, 1990). Na/K-ATPase activity was measured as a function of Na^+ concentration (0-130 mM) at 20 mm K^+ or as a function of K^+ concentration (0–25 mM) at 120 mM Na^+, as described by Jones *et al.* (2005). ATP affinity (0–3 mM) was determined in the foregoing complete buffer system. Less than 5% of the ATP was hydrolyzed during the assay. Data were analyzed by nonlinear regression using Sigma Plot Graph System 12.5 (Jandel Scientific). Activation curves were fitted according to the Hill model for ligand binding. Michaelis–Menten constants (K_m values) were derived from the Michaelis–Menten equation.

Western blot analyses revealed the persistence of retinoschisin in the enriched plasma membrane fraction of wild-type retinae (Supplemental Figure S6A). Binding of recombinant retinoschisin to murine *Rs1h*$^{-/Y}$ retinal membranes under the different buffer conditions was demonstrated in binding assays (Supplemental Figure S6B) as described in Friedrich *et al.* (2011), with the following modifications: recombinant retinoschisin (1 µg/ml) was applied, and the different Na/K-ATPase test buffers were used for incubation and wash steps.

Measuring cation transport by the retinal Na/K-ATPase in *X. laevis* oocytes via atomic absorption spectrophotometry

Heterologous expression of ATP1A3 and ATP1B2 in *X. laevis* oocytes was achieved using injection of mixtures of complementary RNAs (cRNAs) for both subunits as described (Dürr *et al.*, 2013). To distinguish the activity of the heterologously expressed constructs from the endogenous *Xenopus* Na/K-ATPase, the mutations Q108R and N119D were introduced in the human α3-subunit to reduce the ouabain sensitivity (Price and Lingrel, 1988). The ouabain-insensitive pTLN/ATP1A3 construct was kindly provided by Jan B. Koenderink. The cRNA was prepared by in vitro transcription from pTLN expression constructs harboring ATP1B2 and ATP1A3 cDNA. Oocyte isolation, cRNA injection, heterologous Na/K-ATPase expression in oocytes, and Rb^+ uptake experiments were performed as described in Dürr *et al.* (2013). Rb^+ uptake was assessed with an AAnalyst 800 using the THGA Furnace System and evaluated as described in Dürr *et al.* (2013). Oocytes were incubated for 1 h with or without recombinant retinoschisin (1 or 8 µg/ml) before starting the experiment.

Retinoschisin binding to human retinal Na/K-ATPase comprising the ouabain-insensitive ATP1A3 variant and ATP1B2 was demonstrated after heterologous expression in Hek293 cells as described earlier (Supplemental Figure S6C).

Analysis of signaling pathways in retinal explants

Preparation and treatment of retinal explants are described in Plössl *et al.* (2017). In brief, murine *Rs1h*$^{-/Y}$ retinae at postnatal day 10 were isolated and incubated in 800 µl of medium containing 1 µg of purified retinoschisin or RS1-C59S or equal volumes of control eluate. After 10 or 30 min of incubation at 37°C, retinal explants were removed from medium and processed for subsequent Western blot analysis.

Src kinase inhibitor PP2 and IP3 receptor inhibitor 2-APB were obtained from Sigma- Aldrich and added at a final concentration of 10 or 250 µM, respectively.

SDS–PAGE and Western blot analysis

SDS–PAGE, Western blot analyses, and densitometric quantification of Western blots were performed as previously described (Friedrich *et al.*, 2011; Plössl *et al.*, 2017).

Immunolabeling of retinal cryosections

Enucleation of murine eyes (wild-type mice, postnatal day 10) and fixing, embedding, and cryosectioning were performed as described in Friedrich *et al.* (2011). Immunolabeling was performed as described in Friedrich *et al.* (2011), with antibodies against retinoschisin, Atp1b2, caveolin, Src, Plc, and the IP3 receptor (origin of antibodies; see earlier description), diluted as recommended by the manufacturers. The sections were counterstained with 4′,6-diamidino-2-phenylindol (1:1000; Molecular Probes, Leiden, Netherlands). Images were taken with a custom-made VisiScope CSU-X1 Confocal System (Visitron Systems, Puchheim, Germany) equipped with a high-resolution scientific complementary metal-oxide semiconductor camera (PCO, Kehlheim, Germany) under 40× or 100× magnification. Confocal microscopy pictures were taken with 40× magnification (Supplemental Figure S3) to show the distribution of the proteins across the entire retinal layers, as well as with 100× magnification (Figure 7) to assess putative colocalization with the retinoschisin–Na/K-ATPase complex with the described Na/K-ATPase–associated signal transducers. Using the JACoB plug-in from ImageJ (imagej.nih.gov), the Pearson coefficients (normal and with Costes' randomization), different overlap coefficients (normal, application of manual threshold), and Manders coefficients with manual and Costes' threshold) were

determined over the entire retinal sections from Figure 7 and are given in Supplemental Table S1.

Analysis of Na/K-ATPase localization in retinal explants

Eyes were enucleated from mice at postnatal day 18, and retinae were dissected as described (Hsiau *et al.*, 2007). Retinae were subjected to treatment with retinoschisin, RS1-C59S, and control protein as described (Plössl *et al.*, 2017). Retinal explants were transferred into prewarmed medium (DMEM/Ham's F-12 containing 10% FCS, 100 U/ml antibiotic–antimycotic, 2 mM L-glutamine, and 2 µg/ml insulin, all from Life Technologies), rinsed once in prewarmed medium, and then transferred onto Track Etch Membrane Filters (Whatman, Maidstone, United Kingdom) in 35-mm tissue culture dishes containing 3 ml of medium to which 1 µg of purified retinoschisin, RS1-C59S, or control eluate had been added. The retinal explants on the filters were covered in a small droplet of medium. Cultivation was carried out under sterile conditions in a 37°C incubator with a 5% CO_2 environment. Medium was replaced every 36 h, and total cultivation time was 1 wk. Subsequently the retinal explants were fixed, cryopreserved, and cut into 10-µm sections for subsequent histological analyses using antibodies against retinoschisin and Atp1a3 as described.

ACKNOWLEDGMENTS

We thank Lisa Parakenings and Denise Schmied (Institute of Human Genetics, University of Regensburg, Regensburg, Germany) for excellent technical assistance and Jan B. Koenderink (Department of Pharmacology and Toxicology, Nijmegen University, Netherlands) for providing the ATP1A3 expression clone for oocyte experiments. We thank Antje Grosche (Institute of Human Genetics, University of Regensburg) for access to and help with the confocal microscope, which is funded by INST 89/386-1 FUGG. This work was supported by grants from the Deutsche Forschungsgemeinschaft (FR 3377/1-1) to U.F. and Cluster of Excellence "Unifying Concepts in Catalysis" to T.F. and N.N.T.

REFERENCES

Aizman O, Aperia A (2003). Na,K-ATPase as a signal transducer. Ann NY Acad Sci 986, 489–496.

Aperia AC, Akkuratov EE, Fontana JM, Brismar H (2016). Na+, K+-ATPase, a new class of plasma membrane receptors. Am J Physiol Cell Physiol 310, C491–C495.

Arendt T, Holzer M, Stobe A, Gartner U, Luth HJ, Bruckner MK, Ueberham U (2000). Activated mitogenic signaling induces a process of dedifferentiation in Alzheimer's disease that eventually results in cell death. Ann NY Acad Sci 920, 249–255.

Bai Y, Wu J, Li D, Morgan EE, Liu J, Zhao X, Walsh A, Saikumar J, Tinkel J, Joe B, *et al.* (2016). Differential roles of caveolin-1 in ouabain-induced Na+/K+-ATPase cardiac signaling and contractility. Physiol Genomics 48, 739–748.

Banerjee M, Duan Q, Xie Z (2015). SH2 ligand-like effects of second cytosolic domain of Na/K-ATPase alpha1 subunit on Src kinase. PLoS One 10, e0142119.

Beauge LA, Glynn IM (1979). Occlusion of K ions in the unphosphorylated sodium pump. Nature 280, 510–512.

Berta AI, Boesze-Battaglia K, Magyar A, Szel A, Kiss AL (2011). Localization of caveolin-1 and c-src in mature and differentiating photoreceptors: raft proteins co-distribute with rhodopsin during development. J Mol Histol 42, 523–533.

Cali T, Ottolini D, Brini M (2013). Calcium and endoplasmic reticulum-mitochondria tethering in neurodegeneration. DNA Cell Biol 32, 140–146.

Cali T, Ottolini D, Brini M (2014). Calcium signaling in Parkinson's disease. Cell Tissue Res 357, 439–454.

Chang L, Karin M (2001). Mammalian MAP kinase signalling cascades. Nature 410, 37–40.

Clifford RJ, Kaplan JH (2013). Human breast tumor cells are more resistant to cardiac glycoside toxicity than non-tumorigenic breast cells. PLoS One 8, e84306.

Cougnon M, Bouyer P, Planelles G, Jaisser F (1998). Does the colonic H,K-ATPase also act as an Na,K-ATPase? Proc Natl Acad Sci USA 95, 6516–6520.

Day NS, Koutz CA, Anderson R (1993). Inositol-1,4,5-trisphosphate receptors in the vertebrate retina. Curr Eye Res 12, 981–992.

Delamere NA, King KL (1992). The influence of cyclic AMP upon Na,K-ATPase activity in rabbit ciliary epithelium. Invest Ophthalmol Vis Sci 33, 430–435.

Desfrere L, Karlsson M, Hiyoshi H, Malmersjo S, Nanou E, Estrada M, Miyakawa A, Lagercrantz H, El Manira A, Lal M, *et al.* (2009). Na,K-ATPase signal transduction triggers CREB activation and dendritic growth. Proc Natl Acad Sci USA 106, 2212–2217.

Dunn KW, Kamocka MM, McDonald JH (2011). A practical guide to evaluating colocalization in biological microscopy. Am J Physiol Cell Physiol 300, C723–C742.

Dürr KL, Tavraz NN, Spiller S, Friedrich T (2013). Measuring cation transport by Na,K- and H,K-ATPase in Xenopus oocytes by atomic absorption spectrophotometry: an alternative to radioisotope assays. J Vis Exp 72, e50201.

Friedrich T, Tavraz NN, Junghans C (2016). ATP1A2 mutations in migraine: seeing through the facets of an ion pump onto the neurobiology of disease. Front Physiol 7, 239.

Friedrich U, Stohr H, Hilfinger D, Loenhardt T, Schachner M, Langmann T, Weber BH (2011). The Na/K-ATPase is obligatory for membrane anchorage of retinoschisin, the protein involved in the pathogenesis of X-linked juvenile retinoschisis. Hum Mol Genet 20, 1132–1142.

Gable ME, Abdallah SL, Najjar SM, Liu L, Askari A (2014). Digitalis-induced cell signaling by the sodium pump: on the relation of Src to Na(+)/K(+)-ATPase. Biochem Biophys Res Commun 446, 1151–1154.

Gartner U, Holzer M, Arendt T (1999). Elevated expression of p21ras is an early event in Alzheimer's disease and precedes neurofibrillary degeneration. Neuroscience 91, 1–5.

Geering K (2006). FXYD proteins: new regulators of Na-K-ATPase. Am J Physiol Ren Physiol 290, F241–F250.

Geering K (2008). Functional roles of Na,K-ATPase subunits. Curr Opin Nephrol Hypertens 17, 526–532.

Gehrig A, Langmann T, Horling F, Janssen A, Bonin M, Walter M, Poths S, Weber BH (2007). Genome-wide expression profiling of the retinoschisin-deficient retina in early postnatal mouse development. Invest Ophtalmol Vis Sci 48, 891–900.

George ND, Yates JR, Bradshaw K, Moore AT (1995). Infantile presentation of X linked retinoschisis. Br J Ophtalmol 79, 653–657.

Golden WC, Martin LJ (2006). Low-dose ouabain protects against excitotoxic apoptosis and up-regulates nuclear Bcl-2 in vivo. Neuroscience 137, 133–144.

Gu X, Reagan A, Yen A, Bhatti F, Cohen AW, Elliott MH (2014). Spatial and temporal localization of caveolin-1 protein in the developing retina. Adv Exp Med Biol 801, 15–21.

Haas M, Wang H, Tian J, Xie Z (2002). Src-mediated inter-receptor cross-talk between the Na+/K+-ATPase and the epidermal growth factor receptor relays the signal from ouabain to mitogen-activated protein kinases. J Biol Chem 277, 18694–18702.

Holasek SS, Wengenack TM, Kandimalla KK, Montano C, Gregor DM, Curran GL, Poduslo JF (2005). Activation of the stress-activated MAP kinase, p38, but not JNK in cortical motor neurons during early presymptomatic stages of amyotrophic lateral sclerosis in transgenic mice. Brain Res 1045, 185–198.

Howard JL, Ridley SM (1990). Acetyl-CoA carboxylase: a rapid novel assay procedure used in conjunction with the preparation of enzyme from maize leaves. FEBS Lett 261, 261–264.

Hsiau TH, Diaconu C, Myers CA, Lee J, Cepko CL, Corbo JC (2007). The cis-regulatory logic of the mammalian photoreceptor transcriptional network. PLoS One 2, e643.

Illario M, Cavallo AL, Bayer KU, Di Matola T, Fenzi G, Rossi G, Vitale M (2003). Calcium/calmodulin-dependent protein kinase II binds to Raf-1 and modulates integrin-stimulated ERK activation. J Biol Chem 278, 45101–45108.

Jones DH, Li T, Arystarkhova E, Barr KJ, Wetzel RK, Peng J, Markham K, Sweadner KJ, Fong GH, Kidder GM (2005). Na,K-ATPase from mice lacking the gamma subunit (FXYD2) exhibits altered Na+ affinity and decreased thermal stability. J Biol Chem 280, 19003–19011.

Khan NW, Jamison JA, Kemp JA, Sieving PA (2001). Analysis of photoreceptor function and inner retinal activity in juvenile X-linked retinoschisis. Vis Res 41, 3931–3942.

Kizhatil K, Sandhu NK, Peachey NS, Bennett V (2009). Ankyrin-B is required for coordinated expression of beta-2-spectrin, the Na/K-ATPase and the Na/Ca exchanger in the inner segment of rod photoreceptors. Exp Eye Res 88, 57–64.

Koenderink JB, Hermsen HP, Swarts HG, Willems PH, De Pont JJ (2000). High-affinity ouabain binding by a chimeric gastric H+,K+-ATPase containing transmembrane hairpins M3-M4 and M5-M6 of the alpha 1-subunit of rat Na+,K+-ATPase. Proc Natl Acad Sci USA 97, 11209–11214.

Kolkova K, Novitskaya V, Pedersen N, Berezin V, Bock E (2000). Neural cell adhesion molecule-stimulated neurite outgrowth depends on activation of protein kinase C and the Ras-mitogen-activated protein kinase pathway. J Neurosci 20, 2238–2246.

Krupinski T, Beitel GJ (2009). Unexpected roles of the Na-K-ATPase and other ion transporters in cell junctions and tubulogenesis. Physiology 24, 192–201.

Laman JD, Schellekens MM, Lewis GK, Moore JP, Matthews TJ, Langedijk JP, Meloen RH, Boersma WJ, Claassen E (1993). A hidden region in the third variable domain of HIV-1 IIIB gp120 identified by a monoclonal antibody. AIDS Res Hum Retroviruses 9, 605–612.

Li X, McClellan ME, Tanito M, Garteiser P, Towner R, Bissig D, Berkowitz BA, Fliesler SJ, Woodruff ML, Fain GL, *et al*. (2012). Loss of caveolin-1 impairs retinal function due to disturbance of subretinal microenvironment. J Biol Chem 287, 16424–16434.

Liang M, Tian J, Liu L, Pierre S, Liu J, Shapiro J, Xie ZJ (2007). Identification of a pool of non-pumping Na/K-ATPase. J Biol Chem 282, 10585–10593.

Liu X, Spicarova Z, Rydholm S, Li J, Brismar H, Aperia A (2008). Ankyrin B modulates the function of Na,K-ATPase/inositol 1,4,5-trisphosphate receptor signaling microdomain. J Biol Chem 283, 11461–11468.

Madan N, Xu Y, Duan Q, Banerjee M, Larre I, Pierre SV, Xie Z (2017). Src-independent ERK signaling through the alpha3 isoform of Na/K-ATPase. Am J Physiol Cell Physiol 312, C222–C232.

McKnight A, Shotton C, Cordell J, Jones I, Simmons G, Clapham PR (1996). Location, exposure, and conservation of neutralizing and nonneutralizing epitopes on human immunodeficiency virus type 2 SU glycoprotein. J Virol 70, 4598–4606.

Miyakawa-Naito A, Uhlen P, Lal M, Aizman O, Mikoshiba K, Brismar H, Zelenin S, Aperia A (2003). Cell signaling microdomain with Na,K-ATPase and inositol 1,4,5-trisphosphate receptor generates calcium oscillations. J Biol Chem 278, 50355–50361.

Mohler PJ, Davis JQ, Bennett V (2005). Ankyrin-B coordinates the Na/K ATPase, Na/Ca exchanger, and InsP3 receptor in a cardiac T-tubule/SR microdomain. PLoS Biol 3, e423.

Molday LL, Hicks D, Sauer CG, Weber BH, Molday RS (2001). Expression of X-linked retinoschisis protein RS1 in photoreceptor and bipolar cells. Invest Ophthalmol Vis Sci 42, 816–825.

Molday LL, Wu WW, Molday RS (2007). Retinoschisin (RS1), the protein encoded by the X-linked retinoschisis gene, is anchored to the surface of retinal photoreceptor and bipolar cells through its interactions with a Na/K ATPase-SARM1 complex. J Biol Chem 282, 32792–32801.

Molday RS, Kellner U, Weber BH (2012). X-linked juvenile retinoschisis: clinical diagnosis, genetic analysis, and molecular mechanisms. Prog Retin Eye Res 31, 195–212.

Morth JP, Pedersen BP, Toustrup-Jensen MS, Sorensen TL, Petersen J, Andersen JP, Vilsen B, Nissen P (2007). Crystal structure of the sodium-potassium pump. Nature 450, 1043–1049.

Ono Y, Tsuruma K, Takata M, Shimazawa M, Hara H (2016). Glycoprotein nonmetastatic melanoma protein B extracellular fragment shows neuroprotective effects and activates the PI3K/Akt and MEK/ERK pathways via the Na+/K+-ATPase. Sci Rep 6, 23241.

Pagenstecher HE (1913). Über eine unter dem Bilde der Netzhautablösung verlaufende, erbliche Erkankung der Retina. Albrecht Von Graefes Arch Klin Exp Ophthalmol 86, 457–462.

Plössl K, Weber B, Friedrich U (2017). The X-linked juvenile retinoschisis protein retinoschisin is a novel regulator of mitogen-activated protein kinase signalling and apoptosis in the retina. J Cell Mol Med 21, 768–780.

Post RL, Hegyvary C, Kume S (1972). Activation by adenosine triphosphate in the phosphorylation kinetics of sodium and potassium ion transport adenosine triphosphatase. J Biol Chem 247, 6530–6540.

Price EM, Lingrel JB (1988). Structure-function relationships in the Na,K-ATPase alpha subunit: site-directed mutagenesis of glutamine-111 to arginine and asparagine-122 to aspartic acid generates a ouabain-resistant enzyme. Biochemistry 27, 8400–8408.

Quintas LE, Pierre SV, Liu L, Bai Y, Liu X, Xie ZJ (2010). Alterations of Na+/K+-ATPase function in caveolin-1 knockout cardiac fibroblasts. J Mol Cell Cardiol 49, 525–531.

Reinhard L, Tidow H, Clausen MJ, Nissen P (2013). Na(+),K (+)-ATPase as a docking station: protein-protein complexes of the Na(+),K (+)-ATPase. Cell Mol Life Sci 70, 205–222.

Rusciano MR, Salzano M, Monaco S, Sapio MR, Illario M, De Falco V, Santoro M, Campiglia P, Pastore L, Fenzi G, *et al*. (2010). The Ca2+-calmodulin-dependent kinase II is activated in papillary thyroid carcinoma (PTC) and mediates cell proliferation stimulated by RET/PTC. Endocr Relat Cancer 17, 113–123.

Sauer CG, Gehrig A, Warneke-Wittstock R, Marquardt A, Ewing CC, Gibson A, Lorenz B, Jurklies B, Weber BH (1997). Positional cloning of the gene associated with X-linked juvenile retinoschisis. Nat Genet 17, 164–170.

Schneider BG, Kraig E (1990). Na+, K(+)-ATPase of the photoreceptor: selective expression of alpha 3 and beta 2 isoforms. Exp Eye Res 51, 553–564.

Sikkink SK, Biswas S, Parry NR, Stanga PE, Trump D (2007). X-linked retinoschisis: an update. J Med Genet 44, 225–232.

Spiller S, Friedrich T (2014). Functional analysis of human Na(+)/K(+)-ATPase familial or sporadic hemiplegic migraine mutations expressed in Xenopus oocytes. World J Biol Chem 5, 240–253.

Takada Y, Fariss RN, Muller M, Bush RA, Rushing EJ, Sieving PA (2006). Retinoschisin expression and localization in rodent and human pineal and consequences of mouse RS1 gene knockout. Mol Vis 12, 1108–1116.

Therien AG, Blostein R (2000). Mechanisms of sodium pump regulation. Am J Physiol Cell Physiol 279, C541–C566.

Tian J, Cai T, Yuan Z, Wang H, Liu L, Haas M, Maksimova E, Huang XY, Xie ZJ (2006). Binding of Src to Na+/K+-ATPase forms a functional signaling complex. Mol Biol Cell 17, 317–326.

Tokhtaeva E, Sun H, Deiss-Yehiely N, Wen Y, Soni PN, Gabrielli NM, Marcus EA, Ridge KM, Sachs G, Vazquez-Levin M, *et al*. (2016). FXYD5 O-glycosylated ectodomain impairs adhesion by disrupting cell-cell trans-dimerization of Na,K-ATPase beta1 subunits. J Cell Sci 129, 2394–2406.

Tolun G, Vijayasarathy C, Huang R, Zeng Y, Li Y, Steven AC, Sieving PA, Heymann JB (2016). Paired octamer rings of retinoschisin suggest a junctional model for cell-cell adhesion in the retina. Proc Natl Acad Sci USA 113, 5287–5292.

Wang H, Haas M, Liang M, Cai T, Tian J, Li S, Xie Z (2004). Ouabain assembles signaling cascades through the caveolar Na+/K+-ATPase. J Biol Chem 279, 17250–17259.

Wang XL, Xing GH, Hong B, Li XM, Zou Y, Zhang XJ, Dong MX (2014). Gastrodin prevents motor deficits and oxidative stress in the MPTP mouse model of Parkinson's disease: involvement of ERK1/2-Nrf2 signaling pathway. Life Sci 114, 77–85.

Weber BHF, Schrewe H, Molday LL, Gehrig A, White KL, Seeliger MW, Jaissle GB, Friedburg C, Tamm E, Molday RS (2002). Inactivation of the murine X-linked juvenile retinoschisis gene, Rs1h, suggests a role of retinoschisin in retinal cell layer organization and synaptic structure. Proc Natl Acad Sci USA 99, 6222–6227.

Weigand KM, Swarts HG, Fedosova NU, Russe FG, Koenderink JB (2012). Na,K-ATPase activity modulates Src activation: a role for ATP/ADP ratio. Biochim Biophys Acta 1818, 1269–1273.

Wu WW, Wong JP, Kast J, Molday RS (2005). RS1, a discoidin domain-containing retinal cell adhesion protein associated with X-linked retinoschisis, exists as a novel disulfide-linked octamer. J Biol Chem 280, 10721–10730.

Xie Z, Askari A (2002). Na(+)/K(+)-ATPase as a signal transducer. Eur J Biochem 269, 2434–2439.

Xie Z, Cai T (2003). Na+-K+–ATPase-mediated signal transduction: from protein interaction to cellular function. Mol Interv 3, 157–168.

Yosef E, Katz A, Peleg Y, Mehlman T, Karlish SJ (2016). Do Src kinase and caveolin interact directly with Na,K-ATPase? J Biol Chem 291, 11736–11750.

Yuan Z, Cai T, Tian J, Ivanov AV, Giovannucci DR, Xie Z (2005). Na/K-ATPase tethers phospholipase C and IP3 receptor into a calcium-regulatory complex. Mol Biol Cell 16, 4034–4045.